

Analysis and Design of a Stabilized Fly Ash as Pavement Base Material

A. Hilmi Lav¹, M. Aysen Lav¹, A. Burak Goktepe²

¹Istanbul Technical University, Faculty of Civil Engineering, 34469, Maslak, Istanbul, Turkey

²Ege University, Department of Civil Engineering, 35100, Bornova, Izmir, Turkey

KEYWORDS: fly ash, cement stabilization, pavement design

ABSTRACT

The main objective of this study is to utilize a class F fly ash as base material in road pavements. Since class F fly ashes do not manifest desirable engineering properties for this purpose, it was decided to stabilize the material with cement. Fly ash may be utilized with or without aggregate as a pavement layer. It should be noted that, in this research only aggregate free stabilized mixtures (fly ash and cement only) were used since the aim was to utilize high volumes of this waste material. Cement content in the stabilized, laboratory prepared samples were between 2%, 4%, 8%, and 10% by total weight. Initially, Texas triaxial test was carried out to justify the suitability of the fly ash as pavement material. Then, mechanical tests were performed to obtain the fundamental properties of the cement stabilized material in order to analyze the pavement structure. Under repeated wheel loading, fatigue cracking is the primary mode of failure of stabilized materials in which cracks initiate due to the repeated tensile stresses. Utilizing an accelerated full scale road test data for the fatigue performance of cement stabilized fly ash and performing a mechanistic-empirical design procedure, required layer thickness for different lives were obtained for different amount of cement content.

INTRODUCTION

The aim of the study presented in this paper is to use a class F fly ash as pavement base material. The most important reason for replacing classical base materials with fly ash is economy and waste utilization. Additionally, fly ash base may continue to increase its strength for a long time due to pozzolanic reactivity. However, class F ashes are not pozzolanic by itself; therefore, in order to be used as a base or subbase course for a road pavement, they should be mixed with a stabilizing agent such as cement or/and lime. Generally, fly ash is also mixed with aggregate in above applications, yet, in this study only aggregate free stabilized mixtures were investigated. Other information regarding various properties of this stabilized material may be found elsewhere^{1,2,3}.

Laboratory tests were the most significant part of this study. The results obtained from the tests such as elasticity modulus, Poisson's ratio and fatigue life performance model were then incorporated into pavement analysis and design procedure to obtain design life vs. layer thickness.

PREPARATION OF SAMPLES

Before starting sample preparation, the moisture-density relationship was determined for each cement content. Compaction was achieved by the standard Proctor procedure and the results are shown in Figure 1. All the samples tested throughout this study were prepared in accordance with the above test results.

TEXAS TRIAXIAL TESTS

The Texas triaxial test is an undrained test, which measures the deformation resistance of pavement layers⁴. The test is carried out using a set of four cylindrical samples having a diameter of 153mm and a height of 203mm. The testing apparatus is a steel cylindrical cell fitted with a rubber membrane on the inside. Air is used to apply lateral pressure between the cell and the membrane. For each sample, a different lateral (constant) stress is applied and vertical stress is increased until the failure is reached. Mohr circles for each lateral stress at failure are drawn on a classification chart to determine the Texas triaxial classification number. Although it is not common practice, the test method is suitable for stabilized materials and they may also be cured before testing to investigate the stabilization effect. In a study by Buihyan, et al⁵, stabilized samples were assessed by the Texas triaxial method after 60 days of curing.

In order to assess the suitability of cement stabilized fly ash as base material, a set of sample containing 2% cement was prepared. The set consisted of four samples and the samples were cured for 7 days. Then, each sample was loaded until failure at different lateral stresses (10 kPa, 30 kPa, 60 kPa, and 90 kPa). The test results indicated that the Texas triaxial classification number is 1.4 for cement stabilized fly ash. NAASRA⁶ states that a Texas triaxial classification number of "3" for a material, indicates that it is likely to perform satisfactorily as a road base and has a design life of around one million equivalent standard axles. According to Texas triaxial test results it was decided that cement stabilized fly ash was suitable as a base material and proceeded further testing. The Texas triaxial test results are presented in Figure 2.

STRENGTH DEVELOPMENT OF CEMENT STABILIZED FLY ASH

Fly ash and cement are called hydraulic binders. That is they can be reactive when mixing with water. As a result of this, there is two types of reactions occur as follows:

- Pozzololanic reaction, namely self-hardening mechanism of fly ash itself
- Reactions result in various hydration products due to cement stabilization

Pozzolanic reaction of Class F fly ashes is not significant, therefore solid bindings between fly ash particles are mainly developed by hydration products due to stabilization. In this study, development of hydration products, namely development of strength of stabilized fly ash was investigated by a Scanning Electron microscope (SEM). It was observed that upon stabilization, there was no evidence of important hydration as can be seen in Figure 3, however, after 7 days the fly ash particles acted as a nucleation and growing sites for hydration products as shown in Figure 4.

Then the following hydration products were identified in cement stabilized fly ash:

- Ettringite was formed using the fly ash spheres as nucleation sites (Figure 5)
- Calcium Silicate Hydrate (C-S-H) gel along with Portlandite [$\text{Ca}(\text{OH})_2$] maintained a bond between particles and ettringite rods joined together, resulting in an increased strength (Figure 6)
- Finally, after 6 months of hydration C-S-H gel had further densified and covered fly ash spheres including the gaps between particles as can be seen in Figure 7 and Figure 8.

RESONANT FREQUENCY TESTS

The resonant-frequency test is basically the excitation of a sample by a vibration generator. The vibration is induced at different bands of frequency. At the moment of resonance, the exciting frequency matches the natural frequency of sample and standing waves are produced. As the natural frequency of a sample is mainly dependent on the fundamental properties of the material (modulus and Poisson's ratio), the resonant-frequency test enables the determination of those properties without damaging the sample.

The aim of conducting this test was essentially to obtain the dynamic Poisson's ratio of stabilized fly ash that will be used both to analyze pavement structure and to calculate the dynamic modulus from the ultrasonic pulse velocity test. The resonant frequency test was unsuitable for the testing of fresh and nonhydrated fly ash samples. Therefore 90 days cured cement stabilized beam samples having a length of 350mm and 100x100mm cross sections were tested. The samples were prepared in a purpose built steel mould and were statically compacted. In computing the dynamic Poisson's ratio, longitudinal and torsional resonant-frequencies must be measured.

The measurements were made by an Erudite resonant-frequency tester⁷. The samples were placed on a special bench, where they were supported at the center nodal point and then clamped by the clamping bar. The longitudinal vibrations were excited placing the couplings (vibration emitter and receiver) at the ends of the sample and the torsional vibrations were produced when couplings were placed to the sides of the sample. Commencing from the low frequency, vibration frequencies for both cases were increased gradually until the outputmeter showed a maximum value, which was the fundamental resonant frequency. The sinusoidal standing wave was also monitored by oscilloscope and the resonant frequency was obtained from the digital frequencymeter. Equations of moduli for longitudinal frequency and torsional frequency are given as follows⁷:

$$E_d = D W n_L^2 \quad (1)$$

$$G_d = B W n_T^2 \quad (2)$$

where,

E_d : Dynamic elasticity modulus (kg/cm^2)

G_d : Dynamic shear modulus (kg/cm^2)

W : Weight of sample (kg)

n_L : Longitudinal resonant frequency (Hz)

n_T : Torsional resonant frequency (Hz)

B, D : Constants related to cross sectional shape and length of sample

From the dynamic elasticity and shear moduli, the dynamic Poisson's ratio was calculated utilizing the following equation and the results of the resonant-frequency test are given in Table 1.

$$\nu_d = (E_d / 2G_d) - 1 \quad (3)$$

ULTRASONIC PULSE VELOCITY TEST

The ultrasonic pulse velocity test is a measurement of the transit time of a longitudinal vibration pulse through a sample, which has a known path length. The test is carried out by applying two transducers (transmitting and receiving) to the opposite end surfaces of the samples. A sufficient acoustical contact between the transducers and the surface of the sample is maintained by a couplant such as silicon grease. The pulse delay between the transducers is measured as the transit time and the ultrasonic pulse velocity is calculated using the length the sample (the distance between the transducers). The ultrasonic pulse velocity method helps to monitor the hydration process that causes the strength increase as a result of a microstructure formation. The ultrasonic pulse velocity time increases over time, that is, the ultrasonic velocity time decreases due to hydration, which gradually increases the stiffness of the material.

In this part of the study, sample preparation, cement contents as well as the dimensions was the same as described in the previous section (350mm in length and a square cross sectional area of 100x100mm). The measurement was carried out according to ASTM C 597⁸, also complying with the RILEM⁹ technical recommendations. A study by Hwang and Shen¹⁰ showed that the pulse velocity is unstable in the first 24 hours of curing. High water content in the material causes instability in the ultrasonic pulse velocity because the pulse passes through the shortest possible path. Therefore, upon preparing the samples an initial measurement was made across the width (100mm) instead of the length (350mm) and a further measurement was taken after 24 hours. According to the results as shown in Figure 9, hydration started to form soon after the preparation (although it is not significant in Figure 3). Besides, the dynamic elasticity modulus was calculated from the following relation⁹:

$$E_d = \rho v_u^2 [(1 + \nu_d) (1 - 2 \nu_d)] / (1 + \nu_d) \quad (4)$$

where, ν_d is dynamic Poisson's ratio, ρ (kg/m³) is density, and v_u (m/s) is ultrasonic pulse velocity. The dynamic Poisson's ratio was determined by the resonant frequency test mentioned in the previous section.

The increase of dynamic modulus, which corresponds to the increase in the ultrasonic pulse velocity, indicated that cement stabilization is successful in terms of initial setting. Initial setting is important in pavement projects because the road is usually expected to be open for service as soon as possible. Furthermore, at the construction stage, the pavement may be subjected to higher stresses because of heavy trucks and road construction machinery. Therefore, in order to avoid excessive damage, early development of elastic stiffness and strength has always been desirable in stabilization projects. Even though the moduli of all the samples were almost the same upon compaction, after one day the samples increased their modulus as much as five times. The gap then started to decrease and at 28 days, when the hydration rate of cement had slowed. The dynamic modulus of cement stabilized fly ash is presented in Figure 10.

FAILURE MECHANISM OF STABILIZED FLY ASH

The Accelerated Loading Facility (ALF) is a mobile road testing machine. The ALF was designed and manufactured by the Roads and Traffic Authority (RTA), New South Wales. Since 1984, the machine has been owned and operated by the Australian Road Research Board (ARRB). Also, the US Federal Highway Administration purchased the manufacturing rights and constructed the machine in 1986. Another ALF was manufactured by the RTA for the Research Institute of Highway, China. The machine applies full scale half axle wheel loading at a constant speed of 20 km/h to a pavement test strip of 12 m. The load wheel assembly is guided by a main frame and the loading can either be applied over a normal transverse distribution of 1.4 m, 1 m or channelized. The load is applied in one direction alone and after each cycle, the wheel lifted off the pavement and returned back to the starting point through the main frame. The wheel load can be varied between 40 and 80 kN, in 10 kN increments. In this study, an ALF trial results were used to characterize fatigue performance of cement stabilized fly ash.

Basically, stabilized materials have two modes of failure under repeated wheel loading. Fatigue cracking which is the primary mode of failure initiates at the bottom of the stabilized layer due to the tensile stress. The other is crushing and fracturing of the upper layer due to the vertical compressive and shear stresses. In general, failure of thin stabilized pavements (having a thickness of between 80 - 120 mm) start by fatigue cracking and then punching the cracked parts in to the subbase layer, subsequently crushing of the entire layer. The failure mechanism of relatively thick pavements is crushing of upper parts with less effect on the underlying layers. However, considering all kinds of stabilized pavement materials there is not a unique failure mechanism applicable to every stabilized pavements Therefore, stabilized materials (especially new and unconventional stabilized materials such as fly ash) should be investigated individually¹¹.

ALF testing results showed that, the failure mechanism of stabilized fly ash is fatigue cracking and crushing. The crushing which occurred at the top of the layers was more evident than the fatigue cracking which emerged at the bottom of layers. It was also assumed that the thickness of asphalt layer (top layer) is determinant in the design life and failure mode of cement stabilized fly ash.

PAVEMENT ANALYSIS AND DESIGN

There are basically two design methods available in current practice: Empirical methods and mechanistic-empirical methods. Empirical methods are based on experience gained in practice and from observation of the performance of existing or specially constructed roads under different traffic conditions. One of the first empirical methods was the CBR (California Bearing Ratio) method developed in the 1930's by Hveem and associates. However, the most well known example of the empirical design method is the 1972 version of American Association of Highway Officials' pavement design guide¹² developed in connection with the AASHO road test¹³. The method was based on an equation (prediction model) with coefficients that were statistically obtained from the AASHO test road.

All of the empirical design methods are restricted to the range of pavement materials and traffic loads defined in the procedure. When a new material or different traffic loads outside the range are considered, the empirical methods become insufficient, even unless. As a result

of this, mechanistic-empirical methods take their place. In mechanistic-empirical methods, the first step is to assume the pavement structure and load configuration. Pavement structure may consist of many layers of different materials, but for the general design procedure, the structure is simplified to three distinctly different layers. Such simplification is preferred by many researchers for analyzing various pavements^{14, 15, 16}.

The top layer takes up all the asphaltic concrete, the middle layer can be stabilized material as in this study, and the bottom layer is considered as the subgrade (foundation of the structure). After simplifying the structure, the stress induced by specified wheel loading is calculated in order to identify the critical strains in the structure (pavement analysis) by means of purpose developed computer programs. These programs are usually based on linear elastic theory or finite element methods. The layers in the pavement structure are generally considered to be homogenous and isotropic or cross isotropic. Fundamental properties of layers were expressed by elastic modulus and Poisson's ratio, which can be obtained by laboratory tests.

The critical strains usually occur under the wheel paths. These are the horizontal tensile strains developed at the bottom of both the asphalt layer and stabilized layer, which control fatigue cracking, while the vertical compressive strains at the top of the subgrade, control the permanent deformation as shown in Figure 11. Design criteria for critical strains may be obtained from laboratory tests and full scale trials in terms of number of standard axles. These criteria are the expression of the relationship between allowable strain and the number of load applications to failure as a mathematical equation. The number of standard axles to failure is calculated for each failure mode (fatigue cracking and permanent deformation) with the corresponding critical strains and design criteria. The governing design criterion (the minimum number of load applications to failure) is compared to the design life (the predicted number of equivalent standard axle passing in the life of pavement). If the design life is less than the governing failure criterion in terms of number of standard axles, then the related pavement configuration is considered as satisfactory and acceptable as a valid design. Otherwise, layer thickness and/or material properties are adjusted to reach an acceptable configuration. A schematic illustration of the mechanistic-empirical procedure is given in Figure 12.

ANALYSIS OF STABILIZED FLY ASH PAVEMENT

In this study, a simplified pavement structure having a stabilized fly ash base layer was analyzed for critical strains. The pavement consisted of three layers and the top layer was asphaltic concrete having a thickness of 50mm, a modulus of 2800 MPa, and a Poisson's ratio of 0.40 (since the aim of this study is to assess the stabilized fly ash, other values are assumed). The elastic parameters shown in Table 2 were assigned for stabilized layers. The parameters were derived from laboratory test results discussed previously. The layer thickness varied between 250mm and 500mm to investigate the effect of increasing thickness. The subgrade was assumed to be semi-infinite and analyses were carried out for a variety of modulus values that were designated as CBR. Equivalent standard axle loading (one side dual wheels, 330mm apart, and supporting a load of 4.1 tones with the tire pressure of 700 kPa) was applied throughout the analysis. The assumed pavement structure is given in Figure 13.

Analyses of the pavement structure were performed utilizing three different computer programs to observe the variation of design lives based on layered elastic theory and finite element analysis. CIRCLY¹⁷ and KENLAYER¹⁸ may be applied to layered elastic systems under wheel loadings. These programs are basically based on Burmister's layered elastic

theory. Another program, MICHPAVE¹⁹ which is a nonlinear finite element method (FEM), was also employed; however the pavement structure was assumed linear elastic. Finite element mesh used in this study is given in Figure 14. Calculated maximum tensile strains from each program are given in Table 3. The maximum tensile strains occurred in the cement stabilized layers are found at the bottom of the layer symmetrically between dual wheels and used in design life calculations.

FATIGUE PERFORMANCE AND DESIGN OF STABILIZED FLY ASH PAVEMENT

Fatigue performance of stabilized fly ash was established using the following relationship:

$$N = (a / \mu\epsilon)^b \quad (5)$$

where,

- N : Fatigue life (cycles to failure)
- $\mu\epsilon$: Maximum value of the initial tensile strain (microstrain)
- a, b : Regression coefficients

As mentioned previously, ALF trial test results were used to obtain the above regression coefficients. The results are shown in Table 4. Detailed information regarding full scale trial (ALF trial) may be found elsewhere²⁰. From the maximum calculated strains (Table 3) and fatigue performance relationships (Table 4), design life for a layer of stabilized fly ash can be determined in terms of standard axles as presented in Figures 15 to 17 for different cement contents.

CONCLUSIONS

Cement with fly ash and aggregate have been used as pavement base material for many years, however, in this study, the material did not mix with aggregate. In other words, only aggregate-free stabilized mixtures were used. This type of applications are quite uncommon all around the world, yet in this way significant increase in commercial utilization of this material where authorities desperate to cope with increasing stockpiles, may be achieved.

As can be seen from the design charts, cement content is the most important parameter controlling the design life (fatigue performance) of stabilized layers. It should be stressed that layer thickness is also important on design life. Since the strength of aggregate free stabilized fly ash is lower than the ones mixed with aggregate, cement content and layer thickness should not be less than 8% and 300mm, respectively. Mixes having cement content less than 8% may be used as subbase materials instead of being used in pavement base.

The design lives obtained from CIRCLY and KENLAYER analyses are relatively similar to each other for corresponding cement content and layer thickness, however, there are discrepancies between the design lives obtained from MICHPAVE analyses. Although the pavement structure was assumed linear elastic, calculated maximum tensile strains are relatively low than the corresponding results obtained from CIRCLY and KENLAYER analyses due to the technique employed.

Finally the authors are stressed that, the design charts are given herein as examples only. Various pavement structures may be assumed using the results and relationships arising from this study.

REFERENCES

- [1] Lav, A.H. and Kenny, P.J. 1996a. Utilization of Eraring (NSW) Power Plant Fly Ash as Pavement Base Material, 7th Australia New Zealand Conference on Geomechanics, Adelaide, pp. 655-660.
- [2] Lav, A.H. and Kenny, P.J. 1996b. The Use of Stabilized Fly Ash in Pavements, National Symposium on the Use of Recycled Materials in Engineering Construction, Sydney, pp. 77-81.
- [3] Lav, A.H. and Lav, M.A. 2000. Microstructural Development of Stabilized Fly Ash Pavement Base Material. *Journal of Materials in Civil Engineering*, ASCE, May 2000, pp. 157-163.
- [4] Lay, M.G. 1985. *Source Book for Australian Roads*, ARRB, 533p.
- [5] Bhuiyan, et al. 1995. Evaluation of Calcareous Base Course Material Stabilized with Low Percentage of lime in South Texas, *Transportation research Record*, No 1486, pp. 77-86.
- [6] NAASRA, 1986. *Guide to Stabilization in Roadworks*, 1st Ed. National Association of State Road Authorities, Sydney, 83p.
- [7] ERUDITE, 1990. *Resonant Frequency Tester, Manual*, CNS Electronics Limited, London, 20p.
- [8] ASTM C 597, 1996. *Standard Test Method for Pulse Velocity Thorough Concrete*, American Society for Testing and Materials, Vol. 04.02, pp. 297-299.
- [9] RILEM, 1994. *Technical Recommendations for the Testing and Use of Construction Materials*, International Union of Testing and Research Laboratories for Materials and Construction, E&FN Spon, London, 618p.
- [10] Hwang, C.L. and Shen, D.H. 1991. The effects of Blast-Furnace Slag and Fly Ash on the Hydration of Portland Cement, *Cement and Concrete Research*, Vol.21, pp. 410-425.
- [11] Jameson, G.W. 1995. *Response of Cementitious Pavement Materials to Repeated Loading, Road Rehabilitation by Recycling*, A National Research Project, University of South Australia, 42p.
- [12] AASHTO, 1972. *Interim Guide for Design of Pavement Structures*, American Association of State Highway and Transportation Officials, Washington, D.C.

- [13] HRB,1962. The AASHO Road Test, Report 5: Pavement Research, Special Report 61E,National Academy of Science, National Research Council, Publication 945, Washington, D.C.
- [14] Dormon, G.M. and Edwards, J.M. 1967. Developments in the Application in Practice of a Fundamental Procedure for the Design of Flexible Pavements. Proc. 2nd International Conference on the Design of Asphalt Pavements, pp. 99-107.
- [15] Hadley, W.O., et al. 1973. A Nomographic Design Method for Asphalt Stabilized Pavement Layers, Proc. Of Association of Asphalt Pavement Technologies, Vol.42, pp. 252-275.
- [16] Gerritsen, A.H. and Koole, R.C. 1987. Seven Years' Experience with the Structural Aspects of the Shell Pavement Design Manual, Proc. Of 6th International conference on the Design of Asphalt Pavements, pp. 94-106.
- [17] Wardle, L.J. 1977. Program CIRCLY User's Manual, CSIRO, Division of Applied Geomechanics.
- [18] Huang, Y.H. 1993. Pavement Analysis and Design, Prentice Hall Inc, New Jersey, 805p.
- [19] Harichandran, R.S., Baladi, G.Y., and Yeh, M. 1989. Development of a Computer Program for Design of Pavement Systems Consisting of Bound and Unbound Materials, Department of Civil and Environmental Engineering, Michigan State University.
- [20] Jameson, G. et al., 1996. Performance of Cement-Stabilized Fly Ash Under Accelerated Loading: The Eraring ALF Trial 1995, ARRB TR Contract Report RI 925, 32p.

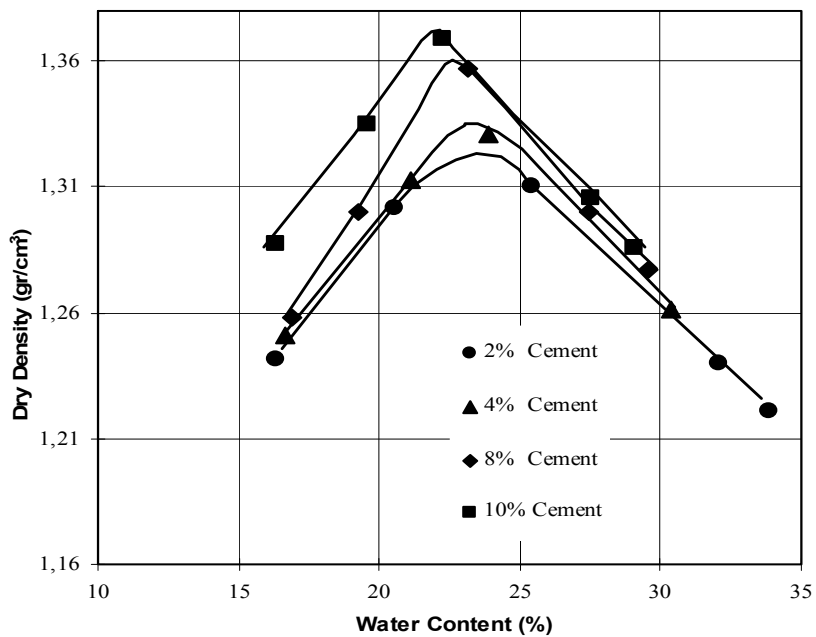


Figure 1. Moisture-Density Relationship of Cement Stabilized Fly Ash

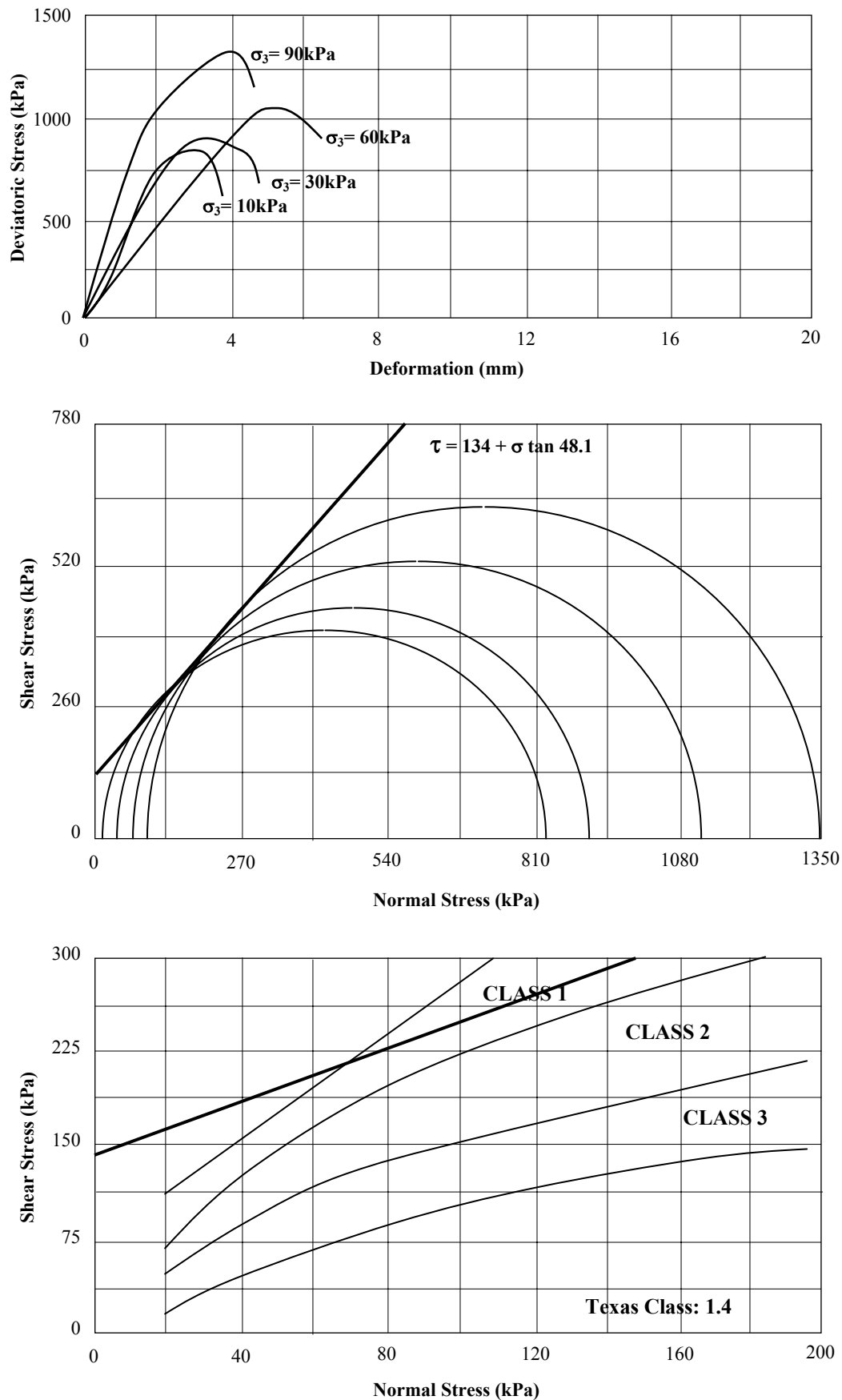


Figure 2 Texas Triaxial Test Results of 2% Cement Stabilized Fly Ash Samples (7 days cure)

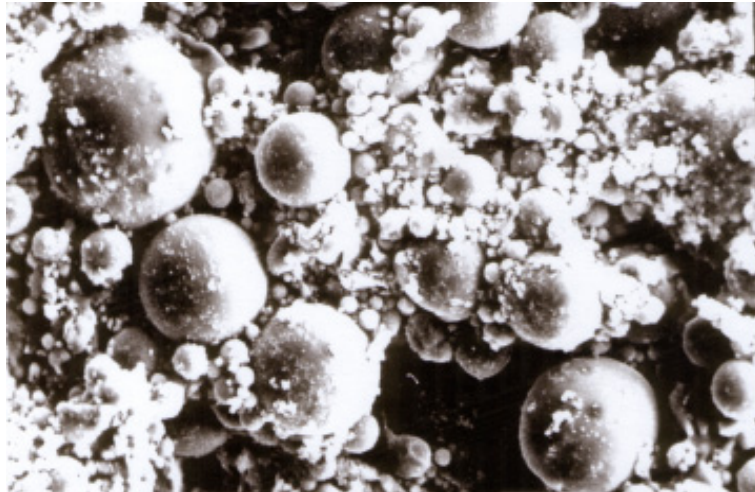


Figure 3 Fly Ash Matrix Upon Stabilization

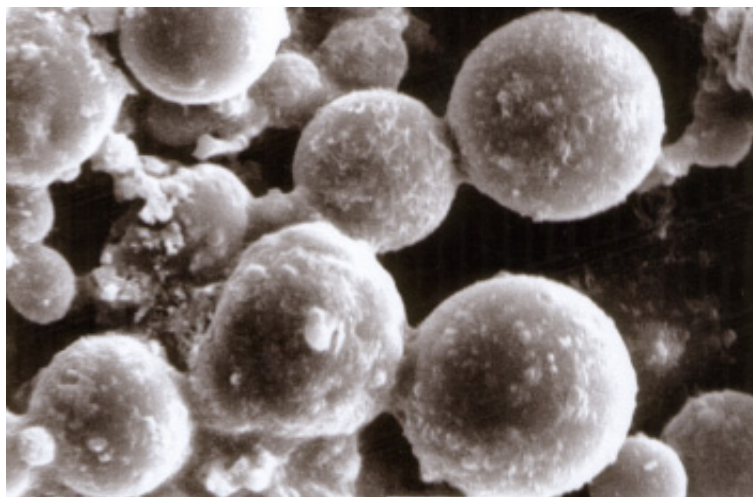


Figure 4 After 7 Days, Fly Ash Particles Acting as a Nucleation and Growing Site

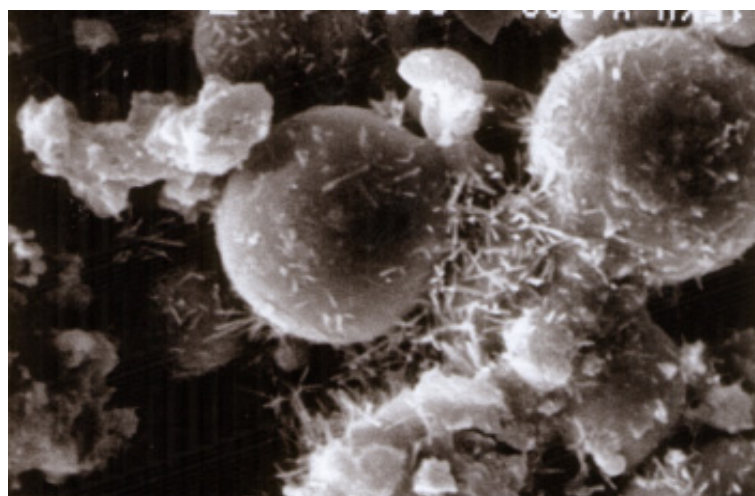


Figure 5 Formation of Ettringite on Fly Ash Spheres

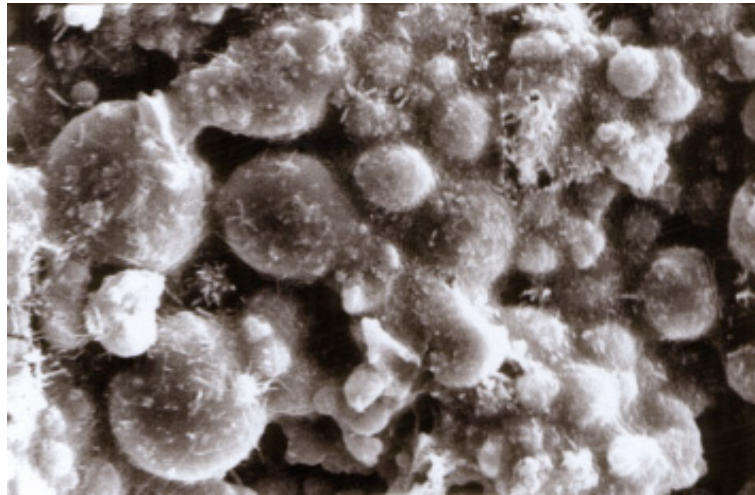


Figure 6 Increase of Bonding Between Fly Ash Particles

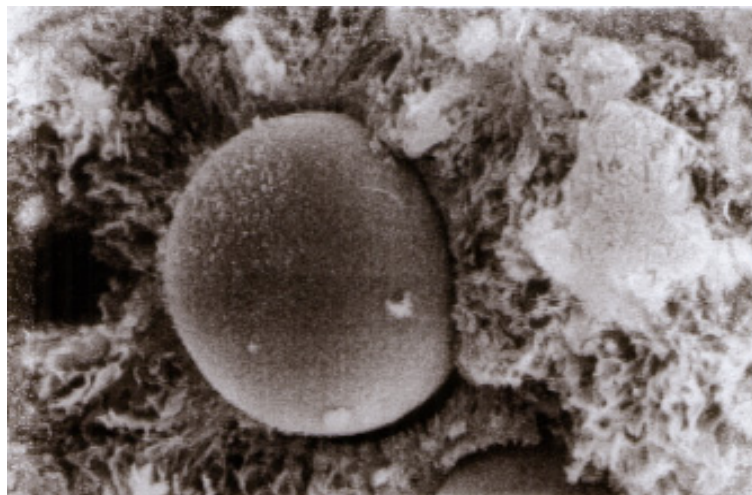


Figure 7 General View of Cement Stabilized Fly Ash After 6 Months of Hydration



Figure 8 Dense C-S-H Gel Around a Fly Ash Sphere After 6 Months

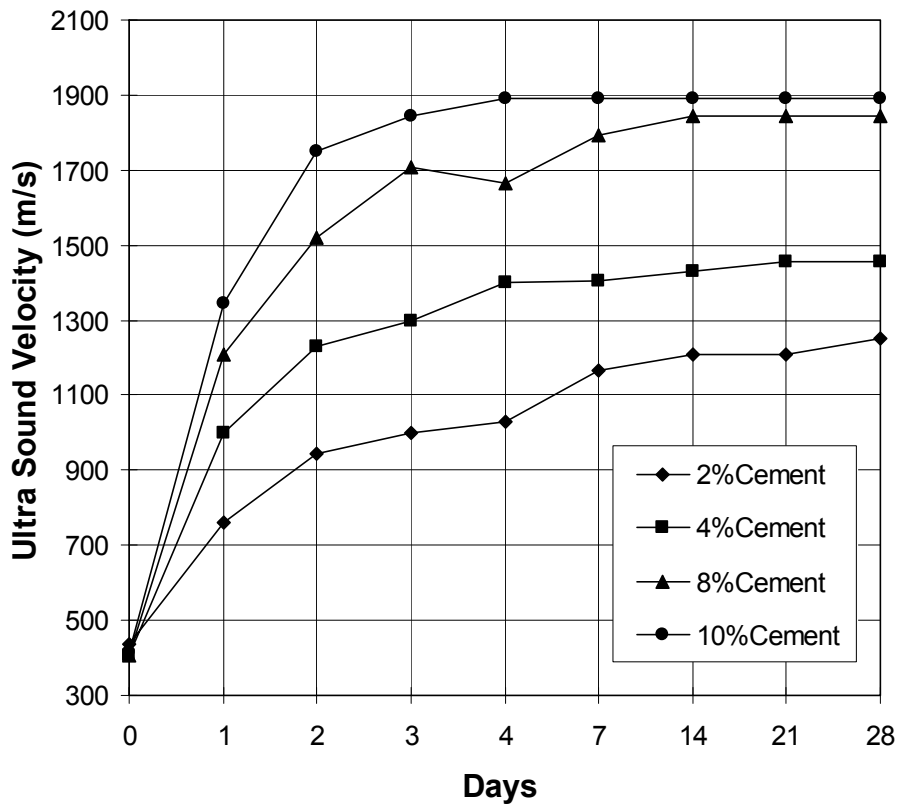


Figure 9 Ultrasonic Pulse Velocity of Cement Stabilized Fly Ash

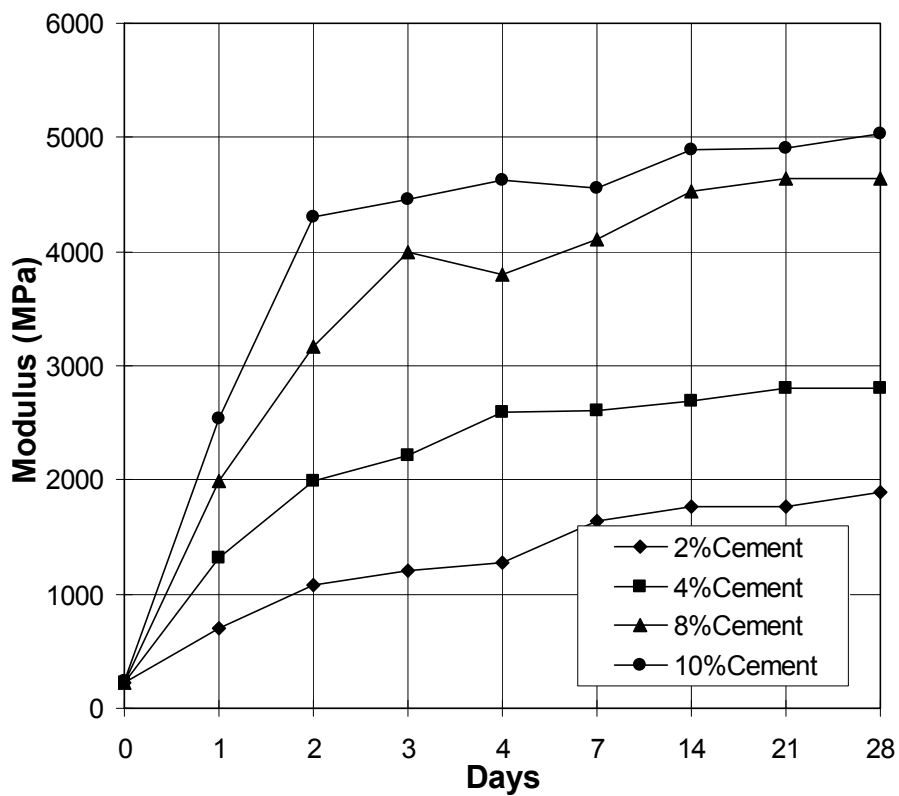


Figure 10 Dynamic Modulus of Cement Stabilized Fly Ash

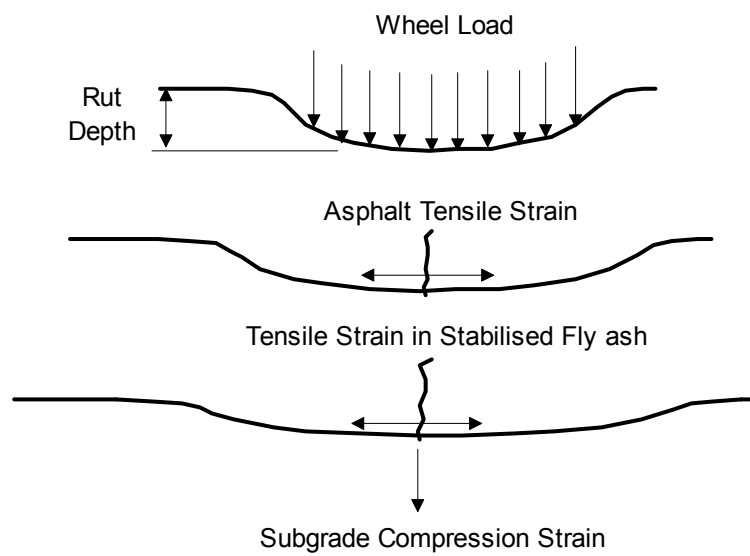


Figure 11 Critical Strains and Failure Mode in Pavement Structures

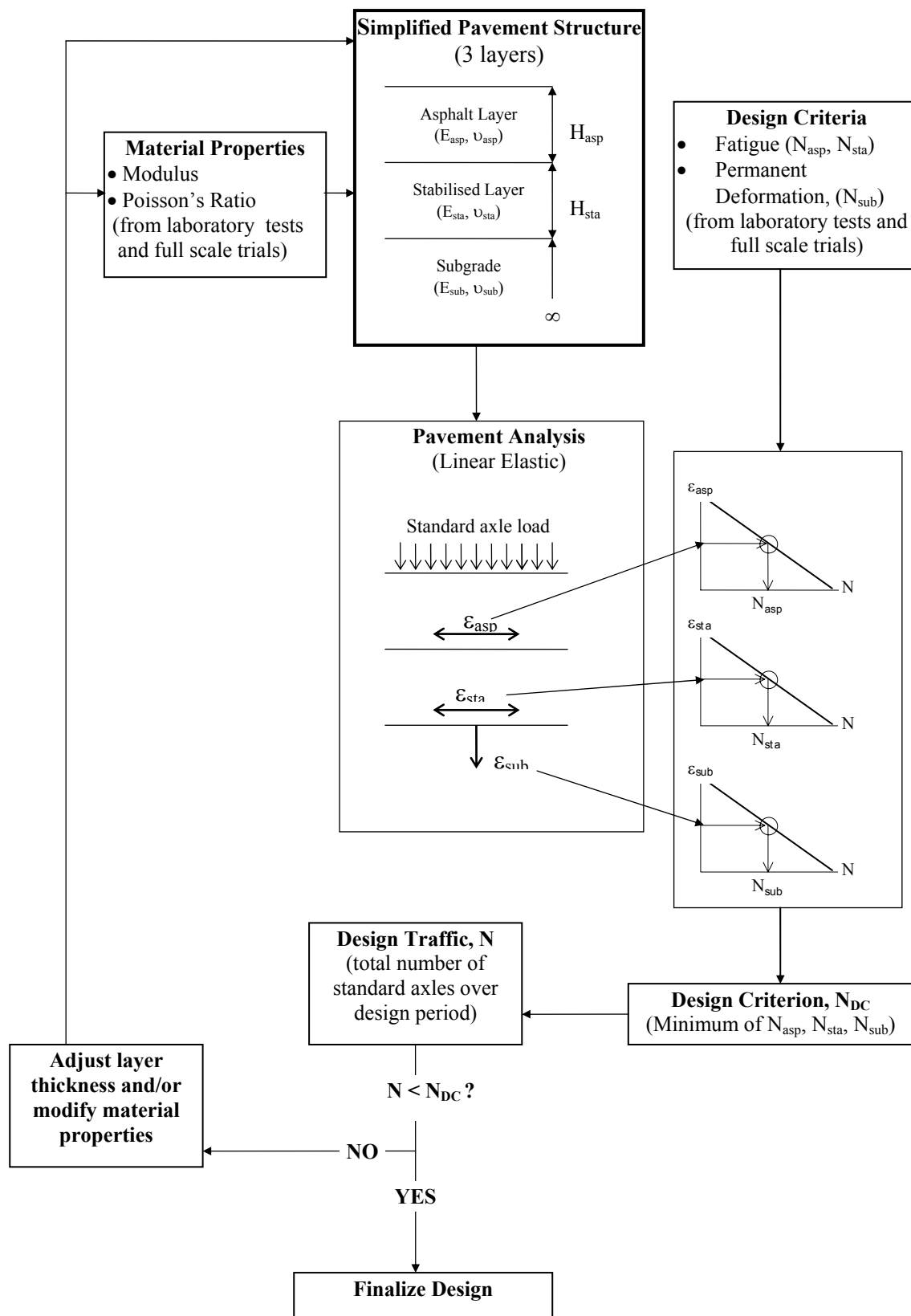


Figure 12 Mechanistic-Empirical Approach to Pavement Analysis and Design

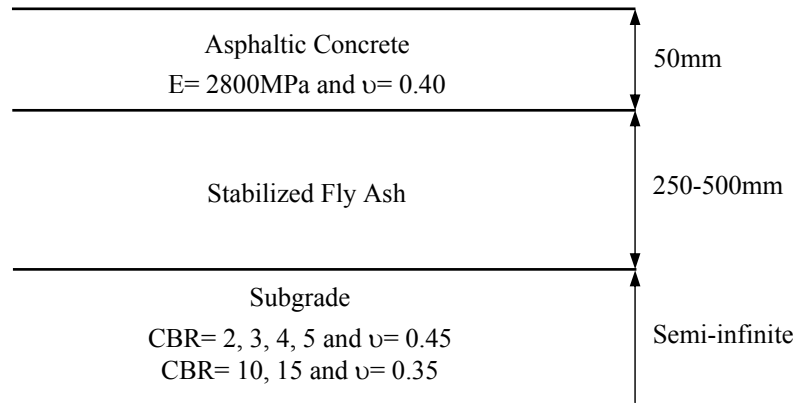


Figure 13. Assumed Pavement Structure Used in the Structural Analyses

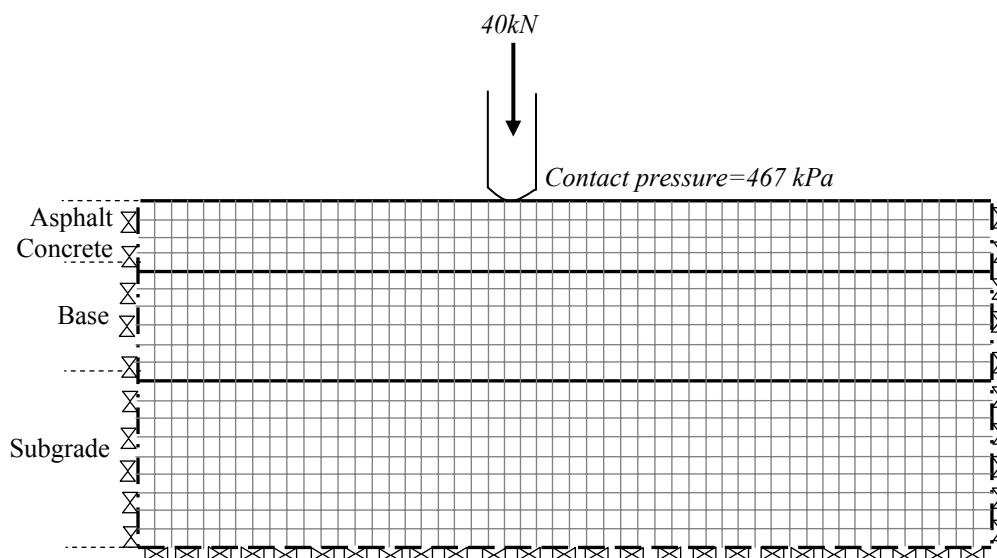


Figure 14. Finite Element Mesh Used in MICHPAVE Analyses

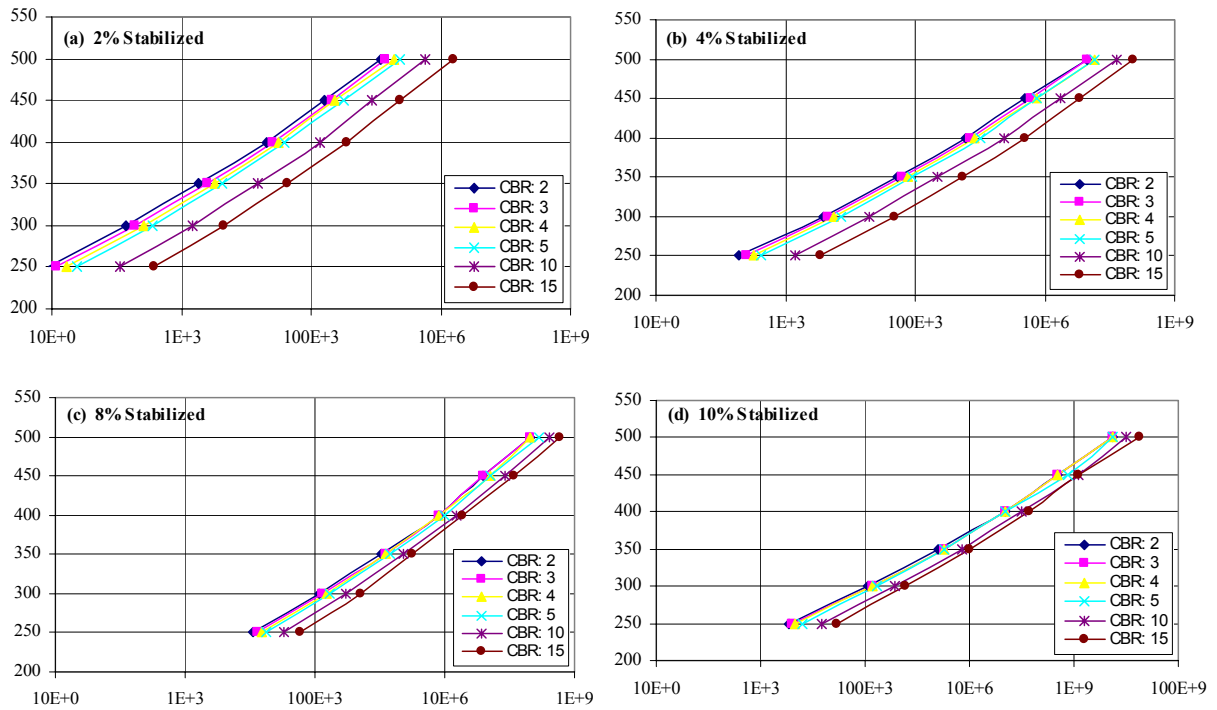


Figure 15. Design Life (fatigue performance) of Stabilized Fly Ash Based on MICHPAVE Analyses

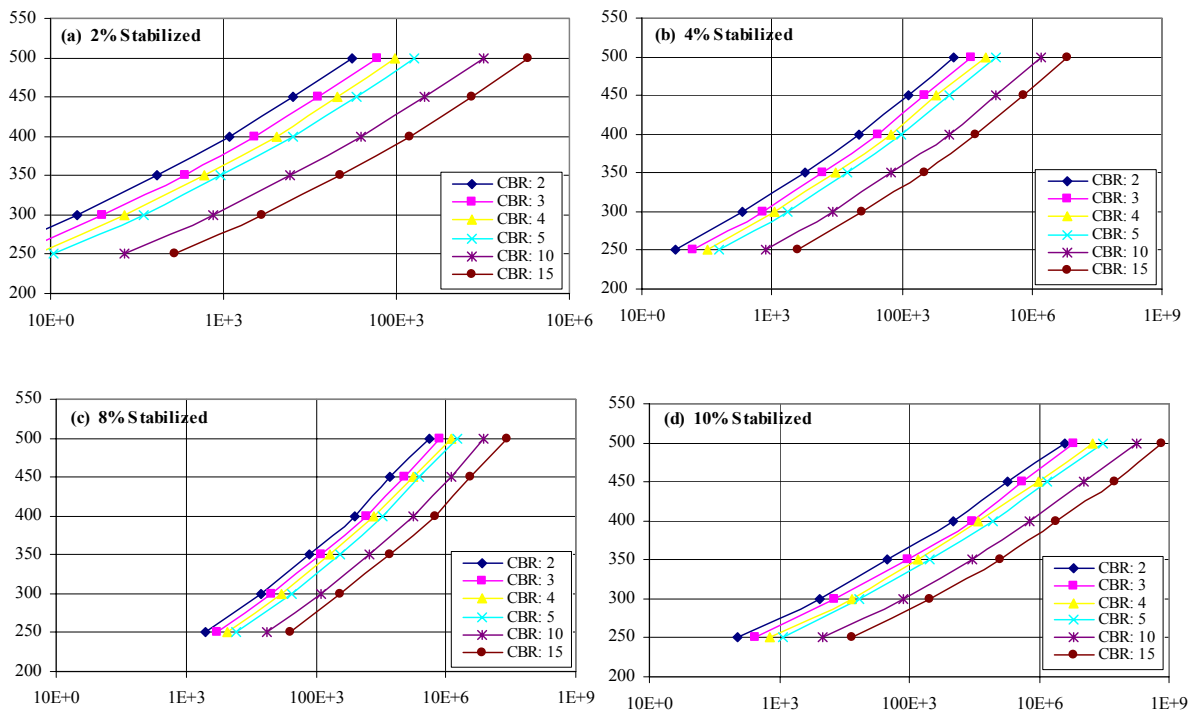


Figure 16. Design Life (fatigue performance) of Stabilized Fly Ash Based on KENLAYER Analyses

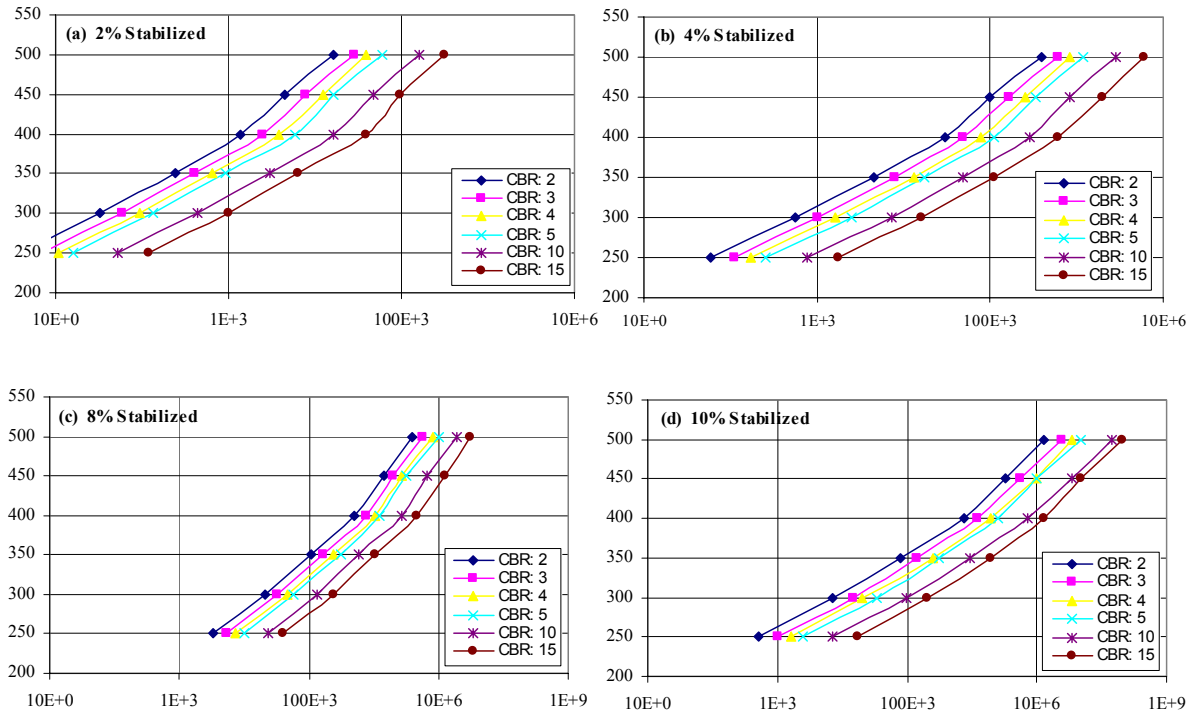


Figure 17. Design Life (fatigue performance) of Stabilized Fly Ash Based on CIRCLY Analyses

Table 1. Resonant-Frequency Test Results

Sample Type	n_L (Hz)	n_T (Hz)	E_d (MPa)	G_d (MPa)	Poisson's Ratio
2% Cement	1657	965	1976	793	0.25
4% Cement	2002	1190	2917	1219	0.20
8% Cement	2624	1573	5086	2163	0.18
10% Cement	2874	1732	6181	2657	0.16

Table 2 Elastic Parameters of Stabilized Fly Ash

Sample Type	Modulus (MPa)	Poisson's Ratio
2% Cement	1500	0.20
4% Cement	2500	0.18
8% Cement	4500	0.16
10% Cement	5600	0.14

Table 3 Calculated Maximum Tensile Strains (Microstrains)

h (mm)	% 2 Cement Stabilized (E= 1500MPa u= 0.20)																	
	CR	MC	KN	CR	MC	KN	CR	MC	KN	CR	MC	KN	CR	MC	KN	CR	MC	KN
250	231	210	248	216	202	229	205	194	216	195	187	204	171	157	165	156	137	142
300	180	153	190	169	148	176	160	143	165	154	138	156	135	118	127	123	104	110
350	144	115	150	136	111	138	129	108	130	124	105	124	109	91	101	100	81	87
400	119	88	121	111	86	112	106	84	105	101	82	100	90	71	82	82	64	71
450	104	70	100	98	68	93	93	67	88	90	65	83	80	58	68	74	52	59
500	90	56	84	85	55	78	82	53	74	78	52	70	70	47	57	65	42	50
CBR	2		3			4			5			10			15			
h (mm)	% 4 Cement Stabilized (E= 2500MPa u= 0.18)																	
	CR	MC	KN	CR	MC	KN	CR	MC	KN	CR	MC	KN	CR	MC	KN	CR	MC	KN
250	162	142	174	151	138	162	144	134	153	138	130	146	122	114	121	111	103	107
300	126	102	133	118	100	123	112	98	117	107	95	111	95	85	93	87	77	83
350	100	76	104	94	75	97	89	73	92	86	72	88	77	65	74	70	59	65
400	81	58	84	77	57	78	73	56	74	70	55	71	63	50	59	58	46	53
450	71	46	69	67	45	65	64	44	62	62	44	59	56	40	49	51	37	44
500	61	36	58	58	36	54	56	35	51	54	35	49	49	32	41	45	30	37
CBR	2		3			4			5			10			15			
h (mm)	% 8 Cement Stabilized (E= 4500MPa u= 0.16)																	
	CR	MC	KN	CR	MC	KN	CR	MC	KN	CR	MC	KN	CR	MC	KN	CR	MC	KN
250	107	90	115	100	88	108	95	86	103	91	84	98	81	77	84	75	71	75
300	82	64	87	77	63	82	73	62	78	71	61	74	63	56	64	58	52	58
350	65	47	68	61	46	64	58	46	61	56	45	58	51	42	50	47	40	45
400	52	35	54	49	35	51	47	35	49	46	34	47	41	32	40	38	31	36
450	45	28	45	43	28	42	41	27	40	40	27	39	36	25	33	33	24	30
500	39	22	37	37	22	35	35	22	33	34	21	32	31	20	28	29	19	25
CBR	2		3			4			5			10			15			
h (mm)	% 10 Cement Stabilized (E= 5600MPa u= 0.14)																	
	CR	MC	KN	CR	MC	KN	CR	MC	KN	CR	MC	KN	CR	MC	KN	CR	MC	KN
250	91	75	99	85	74	93	81	73	88	78	71	84	70	65	73	64	61	66
300	70	53	74	65	52	70	63	52	66	60	51	64	54	47	55	50	45	50
350	55	39	58	52	38	54	49	38	52	48	38	50	43	35	43	40	34	39
400	44	29	46	42	29	43	40	29	42	39	29	40	35	27	35	33	26	32
450	38	23	38	36	23	36	34	23	34	34	22	33	30	21	29	29	21	26
500	33	18	31	31	18	30	30	18	28	29	18	27	26	17	24	25	16	22
CBR	2		3			4			5			10			15			

CR: CIRCLY, MC: MICHPAVE, KN: KENLAYER Computer Programs

Table 4 Regression Coefficients for Fatigue Performance Relationship

Sample Type	a	b
2% Cement	265	9
4% Cement	255	9
8% Cement	340	7
10% Cement	170	10